Available online at www.sciencedirect.com
SCIENCE DIRECT®
Journal of Power Sources 147 (2005) 46–57
JOURNAL OF POWER SOURCES
www.elsevier.com/locate/jpowsour

Review

Sealants for solid oxide fuel cells

Jeffrey W. Fergus *

Auburn University, Materials Research and Education Center, 275 Wilmore Laboratories, Auburn University, AL 36849, USA

Received 1 April 2005; received in revised form 2 May 2005; accepted 4 May 2005
Available online 6 June 2005

Abstract

One of the major challenges for implementation of solid oxide fuel cells (SOFCs) is the development of suitable sealant materials to separate the air and fuel. Several approaches have been used to achieve the necessary adherence, mechanical integrity and stability, including both rigid seals (no applied load during operation) and compressive seals (load applied to seal during operation). The most common approach is to use rigid glass or glass–ceramic seals, the properties of which can be tailored specifically for use in SOFCs through variation of the glass composition. However, these ceramic materials are inherently brittle, so metallic, metallic–ceramic and ceramic–ceramic composite seals, in both the rigid and compressive configurations, have been developed. The use of multiphase seals allows for improvement in factors, such as wettability, compliance at interfaces and strain relief, to improve the gas-tightness and stability of the seal. In this paper, the different approaches for developing SOFC sealants are reviewed.

Keywords: Solid oxide fuel cells; Sealants; Glass–ceramics

Contents

1. Introduction

Planar solid oxide fuel cells (SOFCs) provide higher power density than tubular SOFCs, but require high-temperature sealants, which are not needed in tubular SOFCs [1–6]. The seals must be stable in a wide range of oxygen partial pressure (air and fuel) and be chemically compatible with other fuel cell components, while minimizing thermal stresses during high-temperature operation, and thus create a major challenge in the development of planar SOFCs [7–9]. The quality of the seals must be high, since even small leaks in these seals can affect the cell potential and thus degrade performance [10–11]. The thermal stresses in the seal increase with heating and cooling rate, so the development of sealant materials is particularly important for achieving rapid start-up times [12], which is a major challenge for SOFCs relative to PEM fuel cells. Sealant development is additionally com-

* Tel.: +1 334 844 3405; fax: +1 334 844 3400.
E-mail address: jwfergus@eng.auburn.edu.

0378-7753/$ – see front matter © 2005 Elsevier B.V. All rights reserved.
doi:10.1016/j.jpowsour.2005.05.002

plicated because the optimal sealant depends on the materials used for the other fuel cell components, such as the interconnect alloy [13].

Both rigid and compressive seals are being developed for SOFCs. A major advantage of compressive seals is that the seals are not rigidly fixed to the other SOFC components, so an exact match of thermal expansion is not required. However, maintenance of a gas-tight seal without attaching the components requires the constant application of pressure during operation. Rigid seals, on the other hand, do not require this applied pressure, but have more stringent requirements for adherence, cracking and thermal expansion matching.

2. Rigid seals

2.1. Glass and glass–ceramic sealants

The most common sealants for SOFCs are glass or glass–ceramic materials, and have been shown to operate in fuel cells for more that 1000 h with no significant degradation [14]. Many glasses and glass–ceramics generally used for sealants contain alkali metals [15]. Although some alkali-metal containing glasses have been used for sealants in SOFCs, they are generally avoided because they react with other fuel cell components [16–18] and can enhance the volatility of chromium [19,20], which can lead to poisoning of the cathode. For SOFC applications, alkaline-earth-based glasses are more commonly used.

Two important criteria for selection of a suitable glass sealant are the glass transition temperature (T_g) and the coefficient of thermal expansion (CTE). The glass transition temperature is important because the glass must flow sufficiently to provide an adequate seal, while maintaining sufficient rigidity for mechanical integrity. The softening temperature (T_s) is defined by the viscosity, and is thus a more direct measurement of flow characteristics of the glass. However, the trends in T_s typically follow those for T_g, which is easier to measure, so T_g data is available for a wider range of glass compositions. The coefficient of thermal expansion must match other cell components, such as the yttria-stabilized zirconia (YSZ) electrolyte and the interconnect material, to minimize thermal stresses. The target range for these two criteria suggested by Geassee et al. [21] is shown in Fig. 1, along with corresponding values for glass and glass–ceramic materials investigated for use as SOFC sealants [18,21–28]. The specific compositions that satisfy both criteria are listed in Table 1. Most of the promising compositions are barium-containing glass–ceramics, which have relatively large coefficients of thermal expansion.

Glass–ceramics [29–31] are formed by the deliberate and controlled crystallization of a glass, which typically increases the strength and allows for control of the properties through control of the amount and nature of the crystalline phase(s). In the case of barium-containing glass–ceramics for SOFCs, the crystallization increases thermal expansion. For example, Fig. 2 shows that the coefficients of thermal expansion of $BaO–MgO–SiO_2$ and $BaO–ZnO–SiO_2$ increase with increasing BaO content for constant SiO_2 contents [26]. This increase in coefficient of thermal expansion is due to the formation of barium silicate ($BaSiO_3$), which, as shown in Table 2 [31–36], has a large coefficient of thermal expansion, as compared to, for example, enstatite ($MgSiO_3$). Barium aluminosilicate glass–ceramics crystallize to form celsian ($BaAl_2Si_2O_8$) in addition to, or instead of, barium silicate [20,22,24,25,35]. The two common forms of celsian,

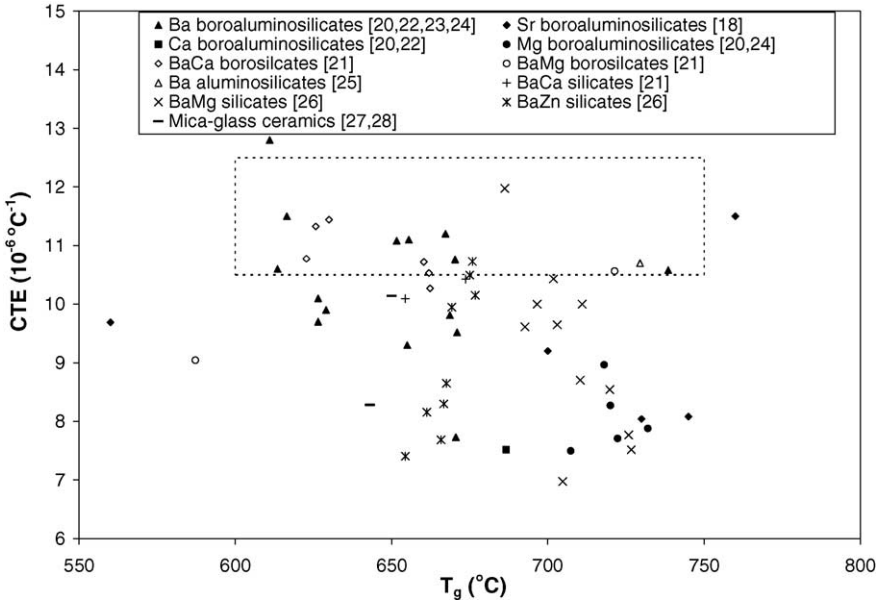

Fig. 1. Glass transition temperatures (T_g) and coefficients of thermal expansion (CTE) for SOFC sealant materials [18,20–28]. The broken line rectangle represents target range suggested by Geasee et al. [21].

Table 1
Glass and glass–ceramic sealants with values of T_g and CTE in target range

Composition (mole%)						Properties		Reference
SiO_2	B_2O_3	Al_2O_3	Alkaline-earth		Other	T_g (°C)	CTE ($°C^{-1} \times 10^6$)	
			BaO/SrO	CaO/MgO				
Boroaluminosilicates								
30	15	10	40 BaO		5 La_2O_3	667	11.2	[23]
38	13	10	35 BaO		5 La_2O_3	739	10.6	
33	17	10	35 BaO		5 La_2O_3	670	10.8	
29	21	10	35 BaO		5 La_2O_3	652	11.1	
33	17	10	35 BaO		5 La_2O_3	656	11.1	[24]
30	22	10	36 BaO		2 ZrO_2	614	10.6	
34	17	10	36 BaO		2 NiO	617	11.5	
Borosilicates								
32	2	0	40 BaO	10 CaO	16 unspecified	660	10.7	[21]
33	3	0	40 BaO	10 CaO	14 unspecified	662	10.5	
31	8	0	38 BaO	15 CaO	8 unspecified	626	11.3	
34	8	0	42 BaO	8 CaO	8 unspecified	623	10.8	
30	7	0	37 BaO	16 CaO	10 unspecified	630	11.4	
Aluminosilicate								
50	0	5	45 BaO			730	10.7	[25]
Silicates								
35	0	0	44 BaO	11 CaO	10 unspecified	721	10.6	[21]
50	0	0	40 BaO	10 MgO		686	12.0	[26]
50	0	0	40 BaO		10 ZnO	676	10.7	
Borate								
8	40	7	25 SrO		20 La_2O_3	760	11.5	[18]

monoclinic and hexagonal, have, as shown in Table 2, very different coefficients of thermal expansion. Hexacelsian provides the high coefficient of thermal expansion needed for SOFC applications, while monocelsian has a very low coefficient of thermal expansion. For some compositions, silica (quartz or cristobablite) can also form [37–39]. Cristobalite is particularly problematic due to a displacive transformation upon cooling with an associated volume decrease, which can cause cracking [38,39]. Strontium forms solid solutions with barium in the celsian crystal

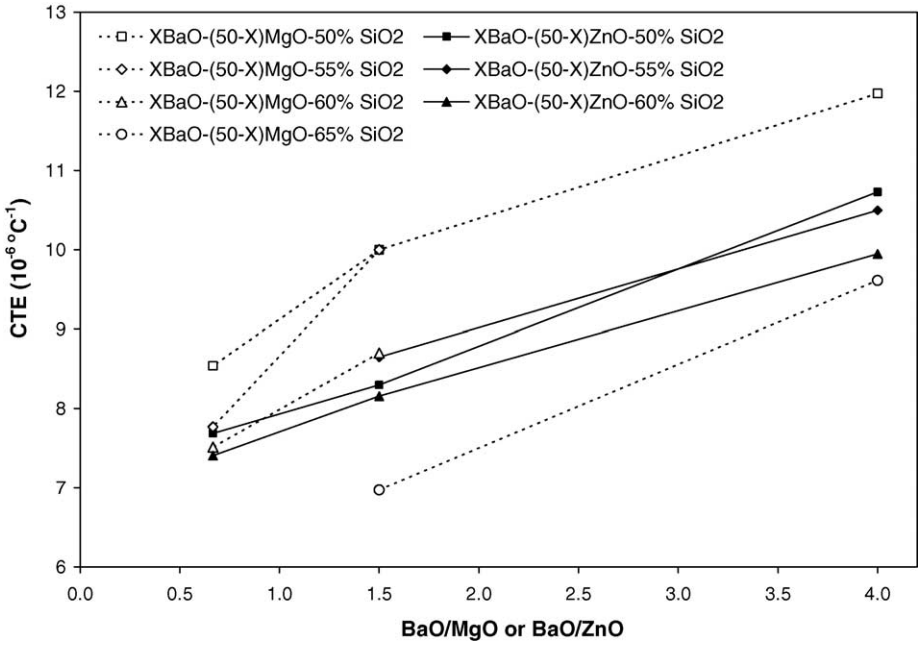

Fig. 2. Effect of barium on the coefficients of thermal expansion (CTE) of BaO–MgO–SiO_2 and BaO–ZnO–SiO_2 glasses [26].

Table 2
Coefficients of thermal expansion of crystalline phases formed in alkaline-earth glass–ceramics

System	Phase	CTE ($°C^{-1} \times 10^6$)	Reference(s)
Mg–Si–O	Enstatite ($MgSiO_3$)	7–9	[31,32]
Ca–Si–O	Wollastonite ($CaSiO_3$)	4–9	[32–34]
	Calcium orthosilicate (Ca_2SiO_4)	10–14	[32,33]
Ba–Si–O	Barium silicate ($BaSiO_3$)	9–13	[33]
	Barium orthosilicate ($BaSi_2O_5$)	14	[33]
Ba–Ca–Si–O	Barium calcium orthosilicate ($Ba_3CaSi_2O_8$)	12–14	[33]
Mg–Al–Si–O	Cordierite ($Mg_2Al_4Si_5O_{18}$)	1	[31,32]
Sr–Al–Si–O	Hexacelsian ($SrAl_2Si_2O_8$)	8–11	[35,36]
	Monocelsian ($SrAl_2Si_2O_8$)	3	[35]
	Orthocelsian ($SrAl_2Si_2O_8$)	5–8	[35,36]
Ba–Al–Si–O	Hexacelsian ($BaAl_2Si_2O_8$)	7–8	[32,33,35]
	Monocelsian ($BaAl_2Si_2O_8$)	2–3	[32,33,35]
	Orthocelsian ($BaAl_2Si_2O_8$)	5–7	[35]

structures and has been shown to stabilize the monocelsian phase [35].

Other alkaline-earth oxides do not dissolve in the celsian phase, but rather form other phases. Calcium oxide is often added to form barium–calcium aluminosilicate (BCAS) sealants, in which case an additional phase, barium calcium orthosilicate phase ($Ba_3CaSi_2O_8$), with a desirably large coefficient of thermal expansion (Table 2), is formed during crystallization [25,33,40–42]. If calcium oxide is used without barium oxide, however, wollastonite ($CaSiO_3$) with [20,22,43] or without [34,44,45] anorthite ($CaAl_2Si_2O_8$) is formed. The addition of magnesium oxide to barium aluminosilicate glass–ceramics results in the formation of enstatite ($MgSiO_3$) and silica along with celsian [38,39]. There is a strong tendency for celsian formation as evidenced by the formation of celsian with only 3% BaO [39] and the presence of only celsian and barium silicate in a glass containing 15% MgO [25]. Magnesium aluminosilicates without barium oxide form cordierite ($Mg_2Al_4Si_5O_{18}$) [20,22,46,47], which, as shown in Table 2, has a very low coefficient of thermal expansion.

While the particular crystalline phases formed in a glass–ceramic are critical to controlling the properties, the crystallization kinetics must also be controlled. The crystallization of barium aluminosilicate glasses is faster than that of the corresponding calcium and magnesium aluminosilicate glasses [20,22,48]. The lower activation energy for crystallization with barium as the network modifier has been attributed to the lower field strength of barium as compared to calcium and magnesium. Thus, barium aluminosilicate glasses crystallize more fully and at lower temperatures as compared to those based on other alkaline-earth cations.

When using a glass–ceramic as a sealant, the glass should wet the surfaces to be bonded or sinter to full density before crystallization, which decreases the viscosity of the glass [16,43,44,50], so the optimal crystallization rate depends on the flow characteristics of the glass [25,26]. If crystallization occurs before complete wetting or sintering occurs, poor adherence or porosity can result. Conversely, insufficient crystallization may lead to inadequate mechanical properties. For example, increasing the length of the crystallization treatment has been shown to increase the rupture strength of a ceramic–metal joint [49]. The crystallization kinetics can be controlled with the addition of nucleating agents. Fig. 3 shows the activation energy for crystallization of magnesium aluminosilicates with some common nucleating agents [20,22,46]. The high activation energy for crystallization with nickel and Cr_2O_3 nucleating agents has been attributed to the more covalent (less ionic) nature of the bonding, which also increases the glass transition temperatures [51]. Control of the crystallization also includes control of the specific phases formed. For example, chromium suppresses the formation of cordierite ($Mg_2Al_4Si_5O_{18}$) [22,51], which as shown in Table 2, has a very low coefficient of thermal expansion. An important distinction among the elements shown in Fig. 3 is that nickel, chromium and titanium can be tetrahedrally coordinated and can thus act as network formers, whereas zirconia is only stable with higher coordination numbers, and thus will only act as a network modifier [51]. Another difference between titania and zirconia, as shown in Fig. 4, is that both titania and zirconia additions lead to a decrease in the coefficient of thermal expansion of magnesium- and barium-based glasses, but, while titania also leads to a decrease in the glass transition temperature, zirconia leads to an increase in the glass transition temperature. Zirconia has also been shown to increase the softening point [24].

Boron oxide is an important addition to silicate glasses. Boron oxide is most commonly added to decrease the viscosity of the glass, and has been shown to decrease the softening point [23,45] and glass transition temperature (Fig. 5 [18,21,23]) of SOFC sealants. Boron oxide also increases the coefficient of thermal expansion, as shown in Fig. 6 for compositions in which only the B_2O_3/SiO_2 ratio is changed [18,23]. However, the effect of boron oxide on the coefficient of thermal expansion is overcome by other alloying additions for more complicated compositions. Fig. 7 shows

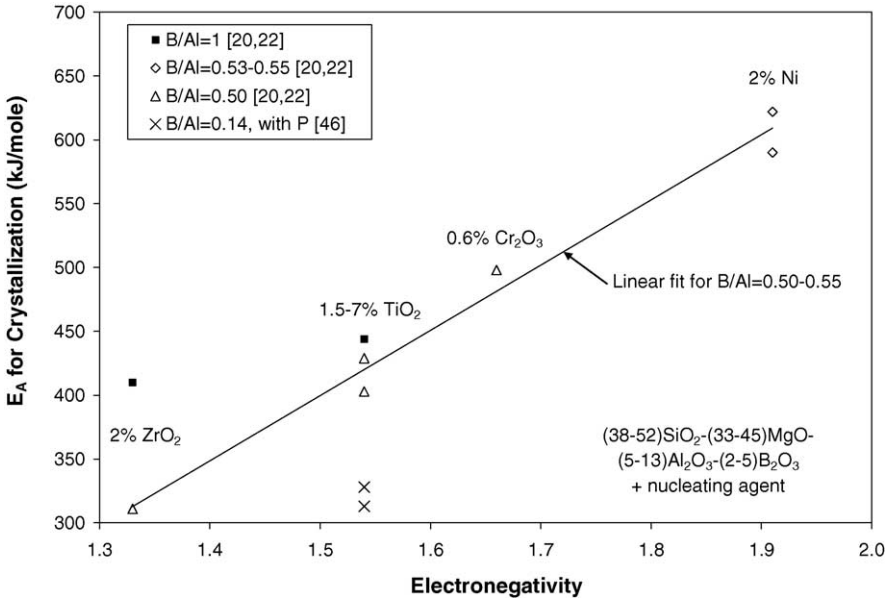

Fig. 3. Activation energy for crystallization (E_A) in glasses containing nucleating agents [20,22,46].

the coefficients of thermal expansion for some of the same glasses shown in Fig. 5. While boron oxide consistently leads to a decrease in the glass transition temperature (Fig. 5), the overall increase in the coefficient of thermal expansion is small compared to the variation in other additions. Fig. 7 also shows the effect of crystallization on the coefficient of thermal expansion. The coefficient of thermal expansion for most of the glasses increases upon crystallization. The exception to this trend is the glass containing magnesium oxide. This trend is consistent with the relative coefficients of thermal expansion for barium- and magnesium-compounds shown in Table 2. Boron oxide also stabilizes the amorphous structure as shown by the increase in activation energy for crystallization with increasing boron content (B/Al ratio) in Fig. 3.

Another important component of glass–ceramics is aluminum, which can have tetrahedral coordination and replace silicon in the glass network, but at larger concentrations acts as a network modifier [30]. This dual role of aluminum has led to reports of aluminum both inhibiting [17,18,50] and enhancing crystallization [22]. Aluminum additions have also been reported to inhibit cristobalite formation [48], which as previously mentioned can cause cracking. Other impor-

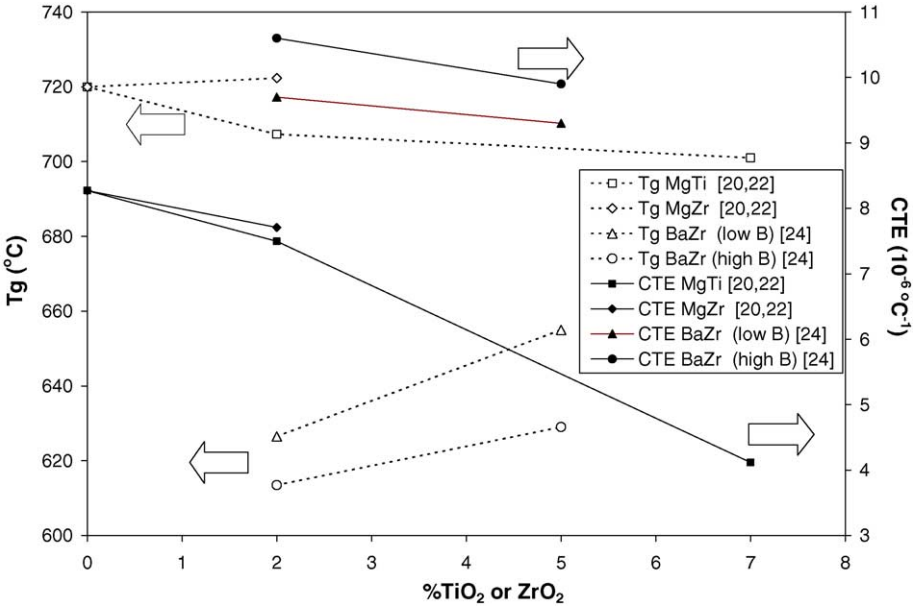

Fig. 4. Effect of TiO_2 and ZrO_2 on the glass transition temperatures (T_g) and coefficients of thermal expansion (CTE) of [20,22,24] of magnesium (MgTi or MgZr) or barium (BaZr) aluminosilicate glass–ceramics.

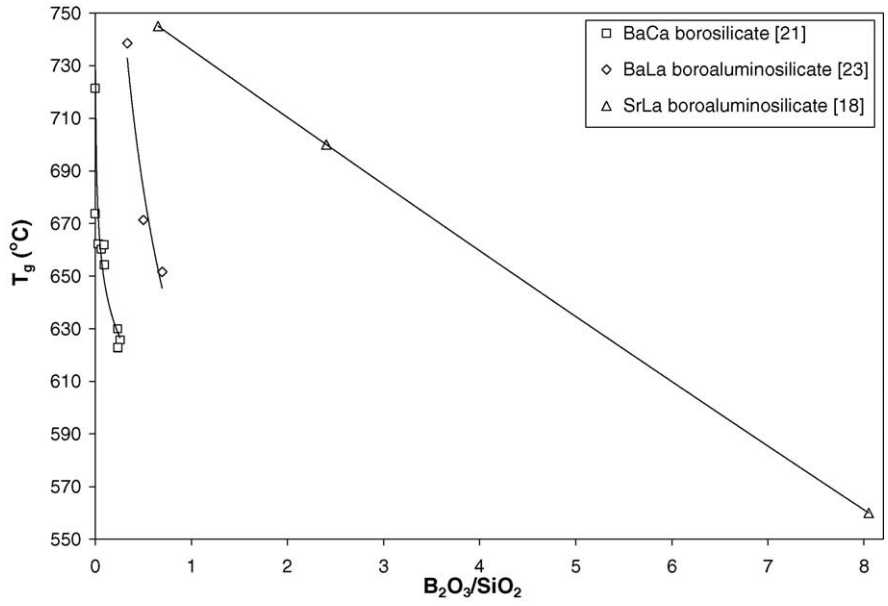

Fig. 5. Effect of B_2O_3 on the glass transition temperatures (T_g) of silicate glasses [18,21,23].

tant additions to glass–ceramics include zinc or lanthanum, which are used to control the viscosity [17,18,50]. Lanthanum additions increase both the softening point [18,24] and the coefficient of thermal expansion [21].

The sealant materials must be chemically compatible with other fuel cell components. The chemical compatibility of glass–ceramic sealants with the yttria-stabilized zirconia electrolyte is generally good. Silicates containing barium [24,45,55], calcium [44,45,52–55] and/or magnesium [54,55] have been reported to form adherent and stable interfaces with yttria-stabilized zirconia. Reactions are more prevalent with the interconnect materials, primarily due to chromium, which is typically present in both ceramic and metallic interconnect materials. Of the commonly used alkaline-earth oxides, silicates containing barium oxide are the most reactive [20,21,48] and those containing magnesium oxide are the most adherent [55]. The interfaces between silicates containing magnesium or calcium and chromium-forming alloys have been observed to contain $MgCrO_4$ [39] or $Ca_3Cr_2Si_2O_8$ [20,48,55], respectively. However, the reaction is more extensive in barium-containing silicates, which, even with the presence of calcium in barium calcium aluminosilicates [20,33,40,41,56–62], form $BaCrO_4$. Thus, the improvements in thermal expansion matching provided by

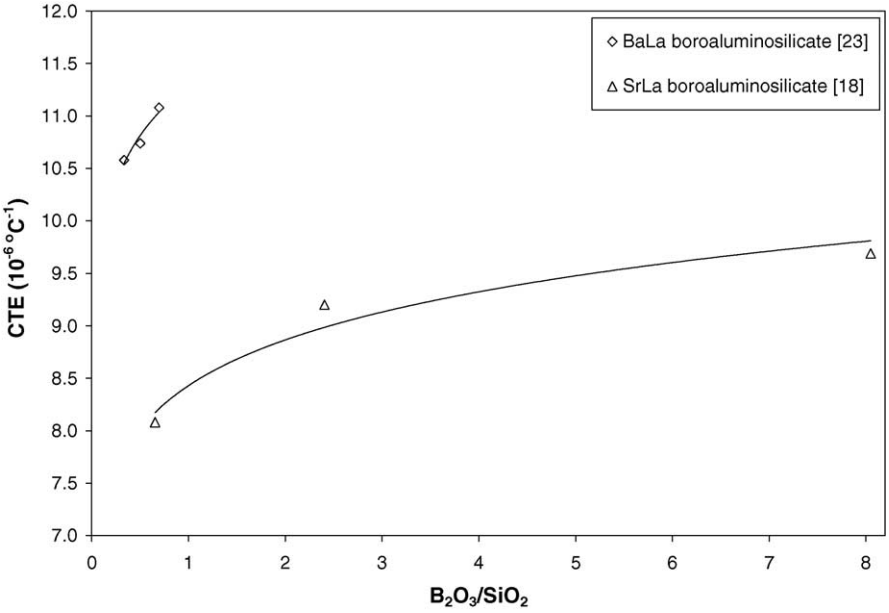

Fig. 6. Effect of B_2O_3 on the coefficients of thermal expansion (CTE) of silicate glasses [18,23].

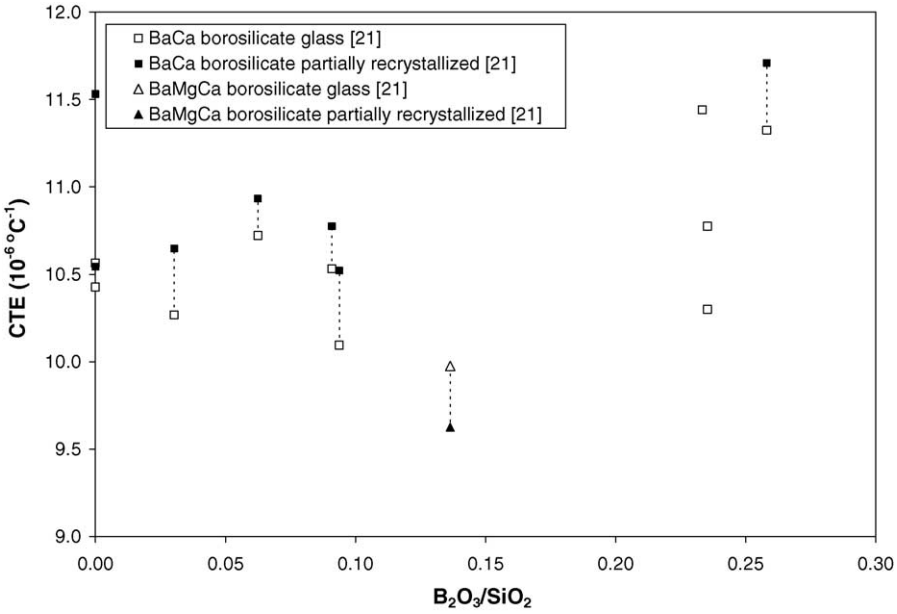

Fig. 7. Effect of B_2O_3 on the coefficients of thermal expansion (CTE) of silicate glasses [21].

barium additions are balanced with increased reaction with the interconnect material. Nonetheless, barium calcium aluminosilicates have been used successfully in operating fuel cells [63]. In addition, the success of glass sealants has led to their use for bonding the interconnects to the frames [64].

Although silicates are the most common ceramic glass sealants, other systems have been investigated. For example, phosphate-based systems have been developed [65–67]. These glasses, however, typically have low coefficients of thermal expansion. Non-oxide systems synthesized from polymer precursors have been developed [68,69]. However, the stability of such systems in the oxidizing environment of the SOFC cathode creates an additional challenge to their implementation.

2.2. Brazes

The other approach to a rigid seal is a metallic braze. Metallic materials have lower stiffness as compared to ceramics and can undergo plastic deformation, both of which allow for accommodation of thermal and mechanical stresses. The sealant is exposed to air, so the braze materials are typically based on metals, such as silver and gold, that are stable in air [70–72]. A major challenge in obtaining a sound metal–ceramic joint is adequate wetting of the ceramic by the braze metal. A common approach to overcoming this challenge is the addition of a reactive metal, such as titanium, which will reduce the oxide and promote wetting. An extreme example of using a reaction to promote bonding is the use of a thermite reaction between aluminum and nickel to bond Fecralloy to yttria-stabilized zirconia [73].

Another approach to improving the wetting characteristics of the braze material is to use a metal + oxide mixture that undergoes an oxide-containing eutectic reaction in air, which improves the wettability of the braze alloy. The Ag–CuO system contains such a eutectic [74,75] and has been used to braze alumina [76] and perovskites [77]. Fig. 8 shows the contact angle for Ag–CuO mixtures with up to 69 mole% CuO on various SOFC components: a yttria (5%)-stabilized zirconia (5YSZ) electrolyte, a FeCrAlY (Fe–22Cr–5Al–0.2Y) interconnect and a LSCF-6428 ($La_{0.6}Sr_{0.4}Co_{0.2}Fe_{0.8}O_{3-\delta}$) cathode [78–80]. The CuO additions are effective for reducing the contact angle on all materials with the largest decrease occurring in the first 10–20 mole% CuO. Fig. 9 shows the strength of joints formed by brazing combinations of the above materials with Ag–CuO [79–80]. There is an initial increase in strength with increasing CuO content, which peaks at around 5–10 mole% CuO and then decreases. The technique was subsequently applied to ferritic stainless steels, including both alumina-forming [81] and chromia-forming [82] steels. The latter joints [82] were exposed to 750 °C for 800 h with no degradation in strength. The joints also held up to 50 cycles to 750 °C with no effect on failure strength, although some delamination of the braze–YSZ joint was observed. There was also evidence of hydrogen dissolving in the braze material and reducing the CuO, although there was no evidence that this adversely affected the strength of the joint.

3. Compressive seals

3.1. Metallic compressive seals

The addition of compression to the seal allows for accommodation of differential thermal expansion between components and can close small gaps to reduce leak rates. For the

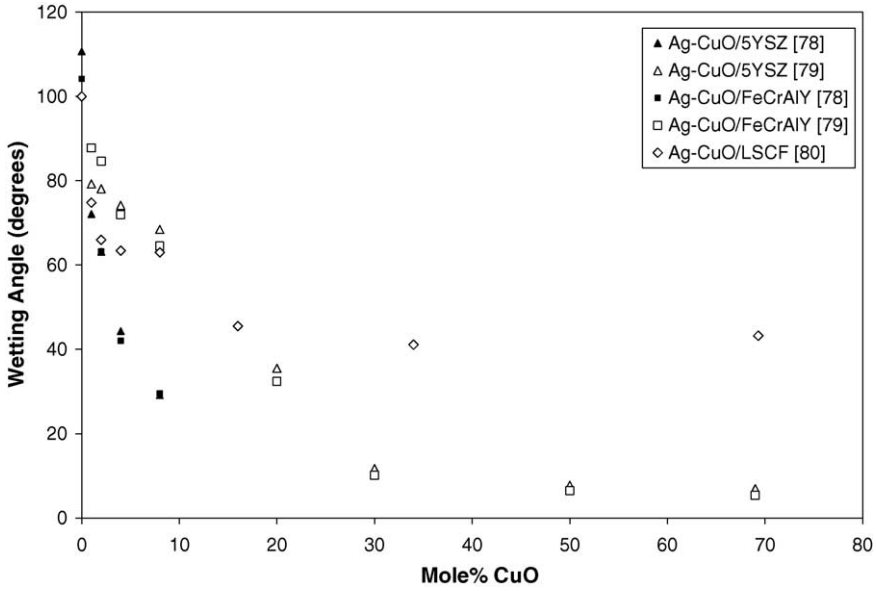

Fig. 8. Wetting angle for Ag–CuO on SOFC electrolyte (5YSZ) [78,79], interconnect (FeCrAlY) [78] and cathode (LSCF) [80] materials.

compression to be effective, however, the seal must deform in response to the applied stress, so one approach is to use ductile metals. To avoid degradation of the seal from the formation of an oxide scale, metals which do not form solid oxides in air, such as gold [83–85] or silver [84–87], are used for metal gaskets in SOFC applications. The strength of metals for metallic seals must fall into a critical range. The strength can be too high, as Duquette and Petric [86] found that sterling silver, with 7.5% copper, had insufficient deformability to provide an adequate seal. On the other hand, Chou and Stevenson [87] found that the leak rate of a silver seal degraded with thermal cycling due to cracking along the grain boundaries. In addition, Singh et al. [88] exposed silver to a dual atmosphere with air on one side and hydrogen on the other. The solubility of both oxygen and hydrogen in silver is significant, so dissolved oxygen from the air side and dissolved hydrogen from the fuel side reacted within the silver to form water and led to failure. This phenomenon must be fully investigated before silver can be used as a sealant in SOFC applications.

Another approach to metallic compressive sealants is to use deformable shapes, which allows for the use of less-deformable metals [84,85]. For example, corrugated or C-shaped gaskets fabricated from superalloys, which are designed to maintain high-temperature strength and oxidation resistance, can maintain a seal due to the pressure applied

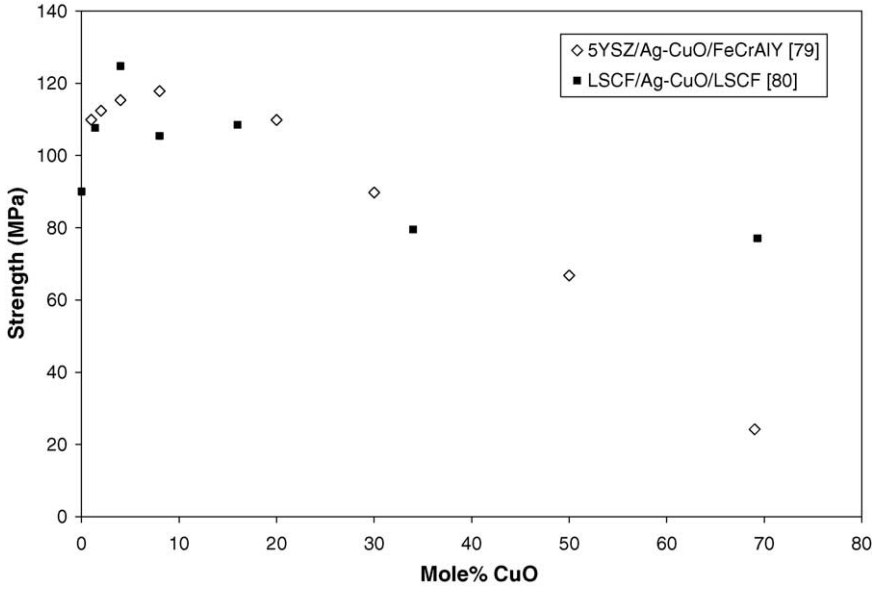

Fig. 9. Strength of YSZ/Ag–CuO/FeCrAlY) [79] and LSCF/Ag–CuO/LSCF [80] joints.

at the interface during elastic deformation of the gasket. The seal from these deformable gaskets can be improved by coating the surface with a ductile metal, which improves the gas-tightness at the interface with a rough surface. Deformable shapes can also be combined with rigid seals by brazing the gasket to the electrolyte and interconnect, in which case, the rigid seal provides the primary seal, but the gasket accommodates some of the strain and thus reduces the stress in the rigid sealant [89].

3.2. Mica-based compressive seals

Another approach to compressive seals is to use mica-based materials [84,87,90–98]. The application of pressure to the overlapping plate-like mica crystals or particles can create a gas-tight seal, as shown schematically in Fig. 10a. In such a seal, the largest source of a leak is typically the interface between the mica and the metal or ceramic, so the seal can be improved through the application of a compliant layer (Fig. 10b), such as a metal or a glass, at the surface of the mica layer, to form what is referred to as a hybrid seal. An alternate method for combining mica and a metal is to place mica powder in the gaps in a corrugated metal seal as shown schematically in Fig. 10c. The seal can be improved further yet, by infiltrating the mica with a phase to improve the sealing between adjacent mica particles. The performance of mica seals are compared in Fig. 11 [84,90–94], which shows the leak rate as a function of applied compressive stress on

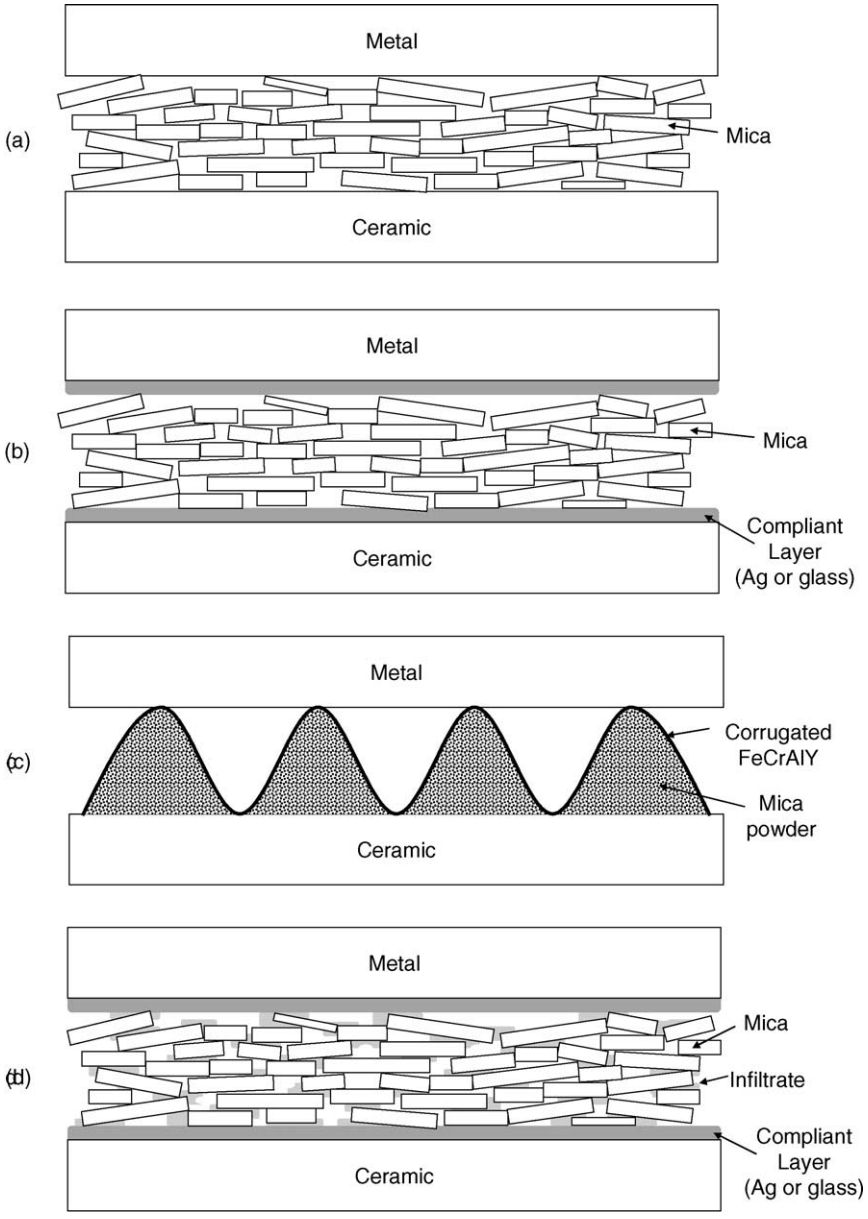

Fig. 10. Mica seals: (a) plain mica seal [91,93], (b) hybrid mica seal with compliant layer (glass or metal) [91,93], (c) mica powder with corrugated alloy [92] and (d) hybrid mica seal with compliant layer and infiltrated mica [94].

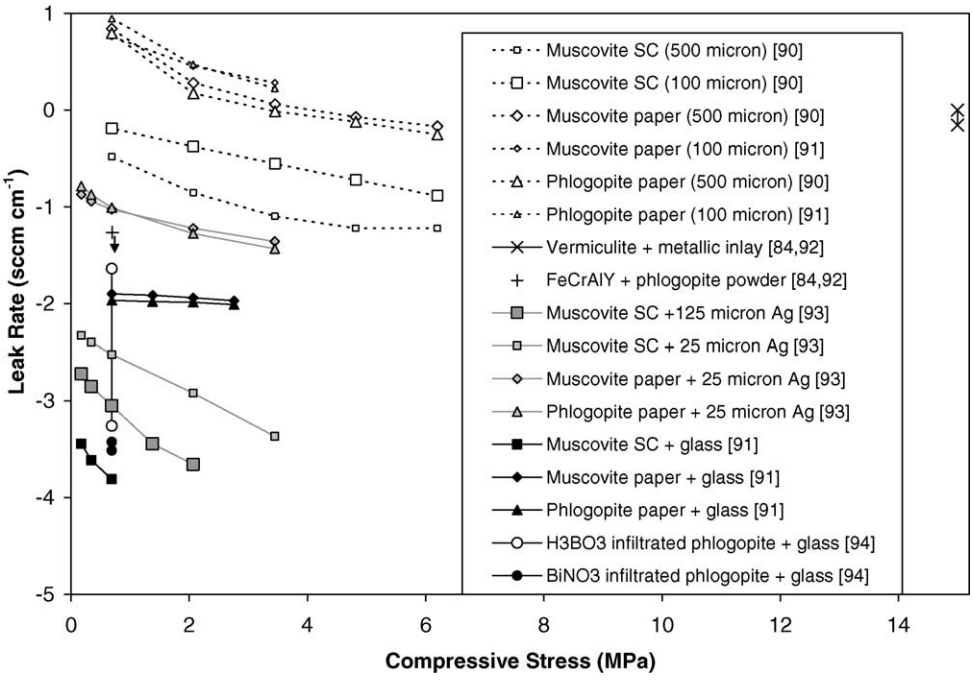

Fig. 11. Leak rates for mica-based seals [84,90–94]. The gas pressure difference across seal is 50 kPa for Bram et al. [84,92] and 14 kPa for Chou et al. [90,91,93,94]. The leak rate for FeCrAlY + phlogopite powder is at the measurable detection limit and thus could be lower as indicated by the arrow.

the joint. One difference among the results shown in Fig. 11 is that the gas pressure difference across the seal used by Bram et al. [84,92] (50 kPa) is higher than that used by Chou et al. [90,91,93,94] (14 kPa).

The two types of mica that have been primarily used for SOFC sealants are muscovite ($KAl_2(AlSi_3O_{10})(F, OH)_2$) and phlogopite ($KMg_3(AlSi_3O_{10})(OH)_2$). The most significant physical difference between the two phases is that the coefficient of thermal expansion of phlogopite is higher than that of muscovite [95]. Two forms of muscovite mica have been tested. One is a cleaved crystal and the other is a mica paper. Phlogopite has been used only in the paper form. The results in Fig. 11 show that the cleaved crystal provides a better seal than the two papers, but the type of mica in the paper does not significantly affect the seal quality. In all cases, the thick layers performed better than thin layers, although the effect of thickness was much greater for the cleaved crystal. The mica layer used by Bram et al. [84,92] was a commercial material, Thermiculite 815™ (Flexitallic, Houston, TX), which is vermiculite mica with a stainless steel inlay.

The use of compliant interlayers decreases the leak rate in all cases. The glass is more effective than the silver for all materials, and the cleaved crystals always provide the best seals. The thickness of the glass compliant layer is not significant (for the thicknesses used), but with the cleaved crystal the 125 μm silver layer is more effective than the 25 μm silver layer. The mica powder with FeCrAlY is in the geometry shown schematically in Fig. 10c. The leak rate shown in Fig. 11 for this seal is at the detectable limit for the experimental apparatus and thus could be lower than that shown in the graph (as indicated by the arrow). The $Bi(NO_3)_3$ infiltrate significantly improves the effectiveness of phlogopite paper (with the glass compliant layer). Although, the initial leak rate is not improved with the H_3BO_3 infiltrate, the leak rate decreases with time, so there is a long-term benefit from the infiltration. The leak rates for the infiltrated paper hybrid seal (glass) approach those of the cleaved crystal hybrid seal (glass), which are the lowest leak rates measured.

The performance of mica-based seals with thermal cycling and with high-temperature exposure has been evaluated. Thermal cycling does not significantly affect the leak rate of seals based on phlogopite paper [95], but does increase the leak rates for seals based on cleaved muscovite crystals (plain and hybrid) [96]. The leak rates of the silver–mica hybrid seals increase and then level off with cycling [87], while the leak rates for infiltrated mica are either unaffected ($Bi(NO_3)_3$)or decrease (H_3BO_3) with cycling [94]. The degradation of mica-based seals at 800 °C is generally minimal [95,97]. However, reaction of steel with Bi_2O_3 in $Bi(NO_3)_3$-infiltrated mica [94] and an increase in leak rate with silver–mica hybrid seals [97] have been observed.

With the application of a glass compliant layer and infiltration of a glass into a mica paper, the resulting material begins to look very much like a glass–ceramic. Mica-based glass–ceramics are available and have been used as sealants for SOFCs. The glass transition temperatures and coefficients of thermal expansion of a few example mica-based glass–ceramics [27,28] are shown in Fig. 1. One of these commercial ceramics, MACOR® (Corning, NY), has been used successfully to bond (without compression) a yttria-stabilized zirconia electrolyte to both metallic (ferritic stainless steel) [99] and ceramic ($La_{0.8}Ca_{0.22}CrO_3$) [27,28]

interconnect materials. However, the MACOR® sealant bonded to the ferritic stainless steel interconnect became discolored when exposed to hydrogen at 900 °C [99] and reacted with the lanthanum chromite interconnect at temperatures of 1000 °C and higher [27,28]. No such reaction has been reported for compressive mica seals at 700–800 °C. This could be due to the lower temperature or to the absence of the potassium-containing glass, which is present in MACOR® [27,28]. Both muscovite and phlogopite contain potassium, but the potassium in the mica structure is likely less reactive than that in the glass matrix. Nonetheless, there are reports of alkali-free mica glass–ceramics [31,100], so if subsequent long-term testing indicates that the potassium in the mica reacts with other fuel cell components, mica-based compressive seals with these alkaline-earth-based (Ba, Sr, Ca) micas can be investigated.

4. Conclusions

Alkaline-earth aluminosilicate glass–ceramics are the most common sealant materials for SOFCs. Although the flow characteristics, thermal expansion behavior and crystallization kinetics of these materials can be controlled with the glass composition, alternative sealing approaches for overcoming the inherent brittleness of glass–ceramic materials are being developed. The most successful alternative approaches are based on composite materials, such as using CuO to improve the wettability, and thus adherence, of a silver braze. Multi-phase ceramic composite layers are also successful, but require an applied compressive load during operation to maintain a gas-tight seal.

References

[1] N.Q. Minh, Solid State Ionics 174 (2004) 271–277.
[2] S.C. Singhal, Solid State Ionics 152–153 (2003) 405–410.
[3] N.Q. Minh, J. Am. Ceram. Soc. 76 (3) (1993) 563–588.
[4] B.C.H. Steele, A. Heinzel, Nature 414 (6861) (2001) 345–352.
[5] S.P.S. Badwal, Solid State Ionics 143 (1) (2001) 39–46.
[6] L.J. Gauckler, D. Beckel, B.E. Buergler, E. Jud, U.P. Muecke, M. Prestat, J.L.M. Rupp, J. Richter, Chimia 58 (12) (2004) 837–850.
[7] A. Khandkar, S. Elangovan, J. Hartvigsen, Ceram. Trans. 65 (1996) 263–277.
[8] H. Yokokawa, N. Sakai, T. Horita, K. Yamaji, Fuel Cells 1 (2) (2001) 117–131.
[9] R.N. Singh, Ceram. Eng. Sci. Proc. 25 (3) (2004) 299–307.
[10] J. Hartvigsen, J. Milliken, S. Elangovan, A. Khandkar, Ceram. Trans. 65 (1996) 279–291.
[11] T. Iwata, Y. Enami, J. Electrochem. Soc. 145 (3) (1998) 931–935.
[12] P. Lamp, J. Tachtler, O. Finkenwirth, S. Mukerjee, S. Shaffer, Fuel Cells 3 (3) (2003) 146–152.
[13] S. Mukerjee, S. Shaffer, J. Zizelman, Proc. Electrochem. Soc. 2003–07 (SOFC VIII) (2003) 88–97.
[14] R. Barfod, S. Koch, Y.-L. Liu, P.H. Larsen, P.V. Hendriksen, Proc. Electrochem. Soc. 2003–07 (SOFC VIII) (2003) 1158–1166.
[15] I.W. Donald, J. Mater. Sci. 28 (11) (1993) 2841–2886.
[16] K.A. Nielsen, M. Solvang, F.W. Poulsen, P.H. Larsen, Ceram. Eng. Sci. Proc. 25 (3) (2004) 309–314.
[17] A. Bieberle, L.J. Gauckler, NATO ASI Series Ser. E: Appl. Sci. 368 (2000) 389–397.
[18] K.L. Ley, M. Krumpelt, R. Kumar, J.H. Meiser, I.D. Bloom, J. Mater. Res. 11 (6) (1996) 1489–1493.
[19] S.P. Jiang, L. Christiansen, B. Hughan, K. Foger, J. Mater. Sci. Lett. 20 (8) (2001) 695–697.
[20] N. Lahl, L. Singheiser, K. Hilpert, K. Singh, D. Bahadur, Proc. Electrochem. Soc. 99-19 (SOFC VI) (1999) 1057–1066.
[21] P. Geasee, T. Schwickert, U. Diekmann, R. Conradt, in: J.G. Heinrich, F. Aldinger (Eds.), Ceramic Materials and Components for Engines, Wiley-VCH Verlag GmbH, Weinheim, Germany, 2001, pp. 57–62.
[22] N. Lahl, K. Singh, L. Singheiser, K. Hilpert, D. Bahadur, J. Mater. Sci. 35 (12) (2000) 3089–3096.
[23] S.-B. Sohn, S.-Y. Choi, G.-H. Kim, H.-S. Song, G.-D. Kim, J. Non-Crystalline Solids 297 (2–3) (2002) 103–112.
[24] S.-B. Sohn, S.-Y. Choi, G.-H. Kim, H.-S. Song, G.-D. Kim, J. Am. Ceram. Soc. 87 (2) (2004) 254–260.
[25] C. Lara, M.J. Pascual, M.O. Prado, A. Durán, Solid State Ionics 170 (3–4) (2004) 201–208.
[26] C. Lara, M.J. Pascual, A. Durán, J. Non-Crystalline Solids 348 (2004) 149–155.
[27] T. Yamamoto, H. Itoh, M. Mori, N. Mori, T. Watanabe, Denki Kagaku Oyobi Kogyo Butsuri Kagaku 64 (6) (1996) 575–581.
[28] T. Yamamoto, H. Itoh, M. Mori, N. Mori, T. Toshi, Proc. Electrochem. Soc. 95-1 (SOFC IV) (1995) 245–254.
[29] R.H. Doremus, Glass Science, second ed., John Wiley & Sons, New York, NY, 1994.
[30] P.W. McMillan, Glass–Ceramics, Academic Press, London, UK, 1979.
[31] W. Höland, G. Beall, Glass–Ceramics Technology, The American Ceramic Society, Westerville, OH, 2002.
[32] Y.S. Touloukian (Ed.), Thermophysical Properties of High Temperature Solid Materials, vol. 4, Oxides and Their Solutions and Mixtures, The MacMillan Co., New York, NY, 1967.
[33] K.S. Weil, J.E. Deibler, J.S. Hardy, D.S. Kim, G.-G. Xia, L.A. Chick, C.A. Coyle, J. Mater. Eng. Perf. 13 (3) (2003) 316–326.
[34] N.H. Menzler, M. Bram, H.P. Buchkremer, D. Stoever, J. Eur. Ceram. Soc. 23 (3) (2002) 445–454.
[35] N.P. Bansal, M.J. Hyatt, C.H. Drummond III, Ceram. Eng. Sci. Proc. 12 (7–8) (1991) 1222–1234.
[36] D. Bahat, J. Mater. Sci. 7 (1972) 198–201.
[37] C. Gunther, G. Hofer, W. Kleinlein, Proc. Electrochem. Soc. 97-40 (SOFC V) (1997) 746–756.
[38] K. Eichler, G. Solow, P. Otschik, W. Schaffrath, J. Eur. Ceram. Soc. 19 (6–7) (1999) 1101–1104.
[39] K. Eichler, G. Solow, P. Otschik, W. Schaffrath, in: A.J. McEvoy (Ed.), European Solid Oxide Fuel Cell Forum Proceedings, vol. 2, The European Fuel Cell Forum, Lucerne, Switzerland, 2000, pp. 899–906.
[40] K.S. Weil, J. Mater. Eng. Perf. 13 (3) (2003) 309–315.
[41] K.S. Weil, Y.Z. Yang, D.M. Paxton, in: J.E. Indacochea (Ed.), Joining of Advanced and Specialty Materials IV, Proceedings of Material Solutions 2001, ASM International, Materials Park, OH, 2002, pp. 69–78.
[42] N.P. Bansal, E.A. Gamble, Proc. Electrochem. Soc. 2005–07 (SOFC IX) (2005) 1932–1941.
[43] S. Ohara, K. Mukai, T. Fukui, Y. Sakaki, M. Hattori, Y. Esaki, J. Ceram. Soc. Japan 109 (2001) 186–190.
[44] Y. Sakaki, M. Hattori, Y. Esaki, Y. Ohara, T. Fukui, K. Kodera, Y. Kubo, Proc. Electrochem. Soc. 97-40 (SOFC V) (1997) 652–660.
[45] R. Zheng, S.R. Wang, H.W. Nie, T.-L. Wen, J. Power Sources 128 (2) (2004) 165–172.
[46] Y.-M. Sung, J. Mater. Sci. 31 (20) (1996) 5421–5427.

[47] S.-B. Sohn, S.-Y. Choi, J. Non-Crystalline Solids 282 (2–3) (2001) 221–227.
[48] N. Lahl, D. Bahadur, K. Singh, L. Singheiser, K. Hilpert, J. Electrochem. Soc. 149 (5) (2002) A607–A614.
[49] J. Malzbender, R.W. Steinbrech, L. Singheiser, J. Mater. Res. 18 (4) (2003) 929–934.
[50] T.W. Kueper, I.D. Bloom, in: K. Natesan, P. Ganesana, G.Y. Lai (Eds.), Heat Resistant Materials II, Conf. Proc. Int. Conf. Heat-Resistant Mater., 2nd, ASM International, Materials Park, OH, 1995, pp. 545–552.
[51] D. Bahadur, N. Lahl, K. Singh, L. Singheiser, K. Hilpert, J. Electrochem. Soc. 151 (4) (2004) A558–A562.
[52] L. Esposito, A. Bellosi, Ceram. Eng. Sci. Proc. 23 (3) (2002) 793–800.
[53] T.-L. Wen, D. Wang, M. Chen, H. Tu, Z. Lu, Z.R. Zhang, H. Nie, Solid State Ionics 148 (3–4) (2002) 513–519.
[54] R.E. Loehman, H.P. Dumm, H. Hofer, Ceram. Eng. Sci. Proc. 23 (3) (2002) 699–710.
[55] T. Schwickert, U. Reisgen, P. Geasee, R. Conradt, J. Adv. Mater. 35 (4) (2003) 44–47.
[56] Z. Yang, K.S. Weil, K.D. Meinhardt, D.M. Paxton, J.W. Stevenson, in: J.E. Indacochea (Ed.), Joining of Advanced and Specialty Materials V, Proceedings of Material Solutions 2002, ASM International, Materials Park, OH, 2003, pp. 40–46.
[57] Z. Yang, K.S. Weil, K.D. Meinhardt, J.W. Stevenson, D.M. Paxton, G.-G. Xia, K.-S. Kim, in: J.E. Indacochea (Ed.), Joining of Advanced and Specialty Materials V, Proceedings of Material Solutions 2002, ASM International, Materials Park, OH, 2003, pp. 116–122.
[58] Z. Yang, J.W. Stevenson, K.D. Meinhardt, Solid State Ionics 160 (3–4) (2003) 213–225.
[59] Z. Yang, K.D. Meinhardt, J.W. Stevenson, J. Electrochem. Soc. 150 (8) (2003) A1095–A1101.
[60] Z. Yang, X. Guanguang, K.D. Meinhardt, K.S. Weil, J.W. Stevenson, J. Mater. Eng. Perf. 13 (3) (2003) 327–334.
[61] V.A.C. Haanappel, V. Shemet, I.C. Vinke, W.J. Quadakkers, J. Power Sources 141 (1) (2005) 102–107.
[62] M. Solvang, K.A. Nielsen, A.R. Dineson, P.H. Larsen, Proc. Electrochem. Soc. 2005–07 (SOFC IX) (2005) 1914–1923.
[63] L.G.J. de Haart, I.C. Vinke, A. Janke, H. Ringel, F. Tietz, Proc. Electrochem. Soc. 2001-16 (SOFC VII) (2001) 111–119.
[64] L. Blum, H.-P. Buchkremer, L.G.J. de Haart, H. Habielek, J.W. Quadakkers, U. Reisgen, R. Steinberger-Wilckens, R.W. Steinbrech, F. Tietz, I. Vinke, Ceram. Eng. Sci. Proc. 25 (3) (2004) 219–227.
[65] P.H. Larsen, P.F. James, J. Mater. Sci. 33 (10) (1998) 2499–2507.
[66] P.H. Larsen, F.W. Poulsen, R.W. Berg, J. Non-Crystalline Solids 244 (1) (1999) 16–24.
[67] R.K. Brow, D.R. Tallant, J. Non-Crystalline Solid 222 (1997) 396–406.
[68] C.A. Lewinsohn, S. Elangovan, S.M. Quist, Ceram. Eng. Sci. Proc. 25 (3) (2004) 315–320.
[69] C.A. Lewinsohn, S. Elangovan, Ceram. Eng. Sci. Proc. 24 (3) (2003) 317–322.
[70] K.S. Weil, J.P. Rice, in: J.E. Indacochea (Ed.), Joining of Advanced and Specialty Materials V, Proceedings of Material Solutions 2002, ASM International, Materials Park, OH, 2003, pp. 123–132.
[71] J.P. Rice, D.M. Paxton, K.S. Weil, Ceram. Eng. Sci. Proc. 23 (3) (2003) 809–816.
[72] T.I. Khan, A. Al-Badri, J. Mater. Sci. 38 (2003) 2483–2488.
[73] J. Mei, P. Xiao, Scripta Mater. 40 (5) (1999) 587–594.
[74] H. Nishiura, R.O. Suzuki, K. Ono, J. Am. Ceram. Soc. 81 (8) (1998) 2181–2187.
[75] R.S. Roth (Ed.), ACerS-NIST Phase Equilibria Diagrams, vol. XIII, The American Ceramic Soc., Westerville, OH, 2001, p. 45 (Fig. 10294).
[76] C.Chr. Schüler, A. Stuck, N. Beck, H. Keser, U. Täck, J. Mater. Sci.: Mater. Electron. 11 (2000) 389–396.
[77] K.M. Erskine, A.M. Meier, S.M. Pilgrim, J. Mater. Sci. 37 (2002) 1705–1709.
[78] K.S. Weil, J.S. Hardy, J.Y. Kim, in: J.E. Indacochea (Ed.), Joining of Advanced and Specialty Materials V, Proceedings of Material Solutions 2002, ASM International, Materials Park, OH, 2003, pp. 47–55.
[79] K.S. Weil, J.Y. Kim, J.S. Hardy, Electrochem. Solid State Lett. 8 (2) (2005) A133–A136.
[80] J.S. Hardy, J.Y. Kim, K.S. Weil, J. Electrochem. Soc. 151 (8) (2004) J43–J49.
[81] K.S. Weil, D.M. Paxton, Ceram. Eng. Sci. Proc. 23 (3) (2002) 785–792.
[82] K.S. Weil, C.A. Coyle, J.T. Darsell, G.G. Xia, J.S. Hardy, J. Power Sources., doi:10.1016/j.jpowsour.2005.01.053.
[83] A. Weber, A. Mueller, D. Herbstritt, W. Ivers-Tiffee, Proc. Electrochem. Soc. 2001–16 (SOFC VII) (2001) 952–962.
[84] M. Bram, S. Reckers, P. Drinovac, J. Moench, R.W. Steinbrech, H.P. Buchkremer, D. Stoever, Proc. Electrochem. Soc. 2003–07 (SOFC VIII) (2003) 888–897.
[85] M. Bram, S.E. Bruenings, F. Meschke, W.A. Meulenberg, H.P. Buchkremer, R.W. Steinbrech, D. Stoever, Proc. Electrochem. Soc. 2001–16 (SOFC VII) (2001) 875–884.
[86] J. Duquette, A. Petric, J. Power Sources 137 (1) (2004) 71–75.
[87] Y.-S. Chou, J.W. Stevenson, J. Mater. Res. 18 (9) (2003) 2243–2250.
[88] P. Singh, Z. Yang, V. Viswanathan, J.W. Stevenson, J. Mater. Eng. Perf. 13 (3) (2003) 287–294.
[89] K.S. Weil, J.S. Hardy, Ceram. Eng. Sci. Proc. 25 (3) (2004) 321–326.
[90] S.P. Simner, J.W. Stevenson, J. Power Sources 102 (1–2) (2001) 310–316.
[91] Y.-S. Chou, J.W. Stevenson, L.A. Chick, J. Power Sources 112 (1) (2002) 130–136.
[92] M. Bram, S. Reckers, P. Drinovac, J. Moench, R.W. Steinbrech, H.P. Buchkremer, D. Stoever, J. Power Sources 138 (1–2) (2004) 111–119.
[93] Y.-S. Chou, J.W. Stevenson, L.A. Chick, J. Am. Ceram. Soc. 86 (6) (2003) 1003–1007.
[94] Y.-S. Chou, J.W. Stevenson, J. Power Sources 135 (1–2) (2004) 72–78.
[95] Y.-S. Chou, J.W. Stevenson, J. Power Sources 124 (2) (2003) 473–478.
[96] Y.-S. Chou, J.W. Stevenson, J. Power Sources 112 (2) (2002) 376–383.
[97] Y.-S. Chou, J.W. Stevenson, J. Power Sources 115 (2) (2003) 274–278.
[98] Y.-S. Chou, J.W. Stevenson, J. Power Sources 140 (2) (2005) 340–345.
[99] R.J. Boersma, N.M. Sammes, Y. Zhang, J. Australas. Ceram. Soc. 34 (1) (1998) 242–247.
[100] S.N. Hoda, G.H. Beall, in: J.H. Simmons, D.R. Uhlmann, G.H. Bell (Eds.), Advances in Ceramics, vol.4, Nucleation and Crystallization in Glasses, American Ceramic Society, Columbus, OH, 1982, pp. 287–300.